Laser Shock-Induced Conformal Transferring of Functional Devices on 3-D Stretchable Substrates

Huang Gao, Rui Tang, Teng Ma, Hanqing Jiang, Hongyu Yu, and Gary J. Cheng

***Abstract*— This paper discussed a top–down integration method to achieve the three-dimensional (3-D) microscale conformal transferring of functional devices on flexible elastomeric substrates at ambient conditions. By the tunable laser-induced pressure, the functional device inherits the microscale wrinkle-like patterns, without compromising functions. The functional materials are encapsulated in the biocompatible parylene layers to avoid the drastic plastic deformations in functional layers. The electrical resistivity of functional device increases marginally with the applied laser intensity, aspect ratios of microscale features, and overall tensile strain applied to the whole flexible assembly. The stretchability of the transferred functional devices was studied by measuring the electrical property as function of bending and tensile strains. It shows that the device can sustain more than 40% strain in the stretchable substrate. It is demonstrated that the process can achieve the flexible and stretchable functional integration conformal to 3-D micrometer-patterns in a fast and scalable way. [2013-0365]**

***Index Terms*— Laser shock, transfer, functional devices, stretchable substrates.**

I. Introduction

AS THE building blocks of modern instruments and equipments for sensing, computation, display and communication, electronic semiconductor components are revolutionized nowadays by two distinct strategies: miniaturization and stretchability/flexibility. While miniaturization improves the computation power in the limited space, systems that are highly bendable, stretchable, conformable to any surface topology, and mechanically robust would greatly expand the horizon of applications. The diversified applications, such as flexible solar cells [1], flexible displays [2], flexible stress sensors [3], wearable electronics [4], as well as medical implants for health monitoring and disease diagnostics [5], have motivated much progress in various fabrication methods of stretchable conductors and devices.

Most of the fabrication methods are bottom-up and categorized into two major strategies, either "stretchable materials" or "stretchable structures" [6]. In the first strategy, the conductive material, such as metals and carbon nano-material, is either dispersed into an elastic matrix to form elastic conductive composites [7] or deposited on the substrate surface [8]. The elastic conductor is readily capable of enduring tensile strain more than 100%, but its conductivity changes or even diminishes when defects and delamination occur at high tensile strains or after fatigue testing. Kim et al., [9] demonstrated stretchable conductors of polyurethane containing spherical nanoparticles deposited by either layer-by-layer assembly or vacuum-assisted flocculation. High conductivity and stretchability were observed in both composites despite the minimal aspect ratio of the nanoparticles. These materials also demonstrate the electronic tunability of mechanical properties, which arise from the dynamic self-organization of the nanoparticles under stress. Our new strategy can directly transfer functional devices conformally onto 3D surfaces of flexible and stretchable substrate, and allow the assembly to inherit stretchability simultaneously. In the second strategy, the brittle devices are bonded onto elastomeric substrates and interconnected by stretchable spring-like ribbons of highly conductive metal or alloy [10]. The ribbons are selectively bonded with elastomeric substrates by surface energy differentiation to form either in-plane serpentines or out-of-plane buckles [11]. The ribbons deform to experience most of stretching and bending so that the brittle devices are almost immune to excessive strains and failure. This strategy requires specially customized microfabrication and metal evaporation technologies, and relatively complicated multiple transfer processes [8]. The maximum strain is usually limited to the range of 20% to 70% due to adhesive failure and interconnection redundancy. In addition, this method can only be applied to materials that could generate buckling under compression. It is still an open topic to demonstrate how to assemble more complicated multilayer devices on microscale 3D-patterned surfaces.

II. Process Scheme

The top-down method proposed in this study, laser shock induced transferring (LST), provides an alternative to selectively fabricate stretchable functional structures conformal to

Manuscript received November 27, 2013; revised May 29, 2014; accepted June 14, 2014. The work of G. J. Cheng was supported in part by the National Science Foundation (NSF) CAREER Award CMMI-0547636, and in part by the NSF through the Materials Processing and Manufacturing Program under Grant CMMI-0928752. The work of H. Jiang was supported in part by the NSF under Grant CMMI-0700440. Subject Editor H. Fujita. *(Corresponding author: Gary J. Cheng.)*

H. Gao and G. J. Cheng are with the School of Industrial Engineering, Purdue University, West Lafayette, IN 47907 USA (e-mail: gao7@purdue.edu; gjcheng@purdue.edu).

R. Tang is with the School of Electrical, Computer, and Energy Engineering, Arizona State University, Tempe, AZ 85287 USA (e-mail: rui.tang.1@asu.edu).

T. Ma and H. Jiang are with the School for Engineering of Matter, Transport, and Energy, Arizona State University, Tempe, AZ 85287 USA (e-mail: teng.ma.1@asu.edu; hanqing.jiang@asu.edu).

H. Yu is with the School of Electrical, Computer, and Energy Engineering, Arizona State University, Tempe, AZ 85287 USA; and is also with the School of Earth and Space Exploration, Arizona State University, Tempe, AZ 85287 USA (e-mail: hongyuyu@asu.edu).

Color versions of one or more of the figures in this paper are available online at http://ieeexplore.ieee.org.

Digital Object Identifier 10.1109/JMEMS.2014.2332512

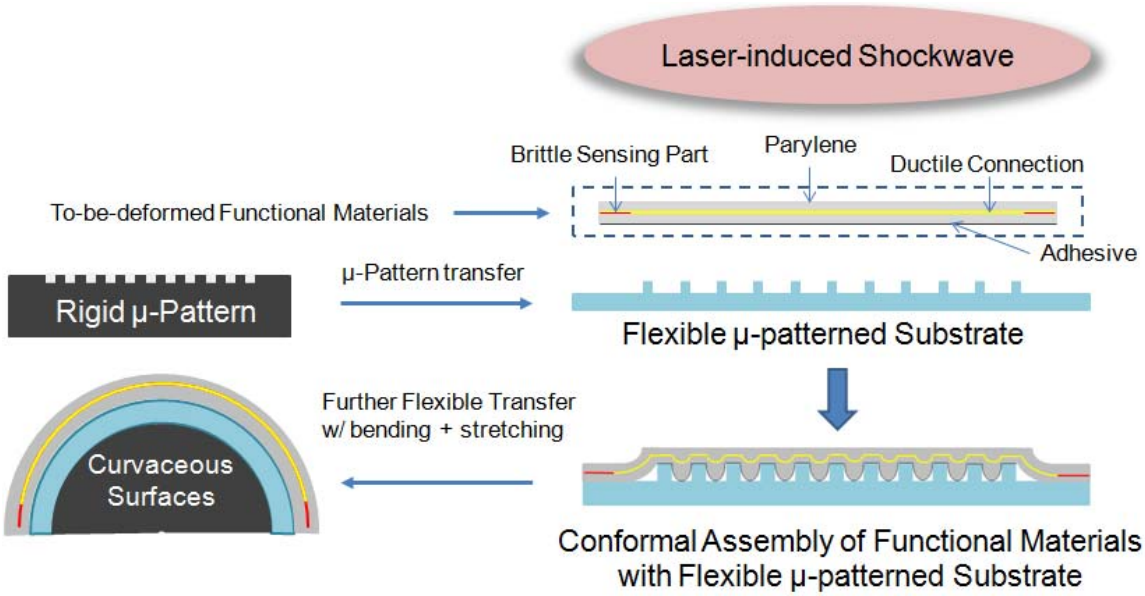

Fig. 1. The process scheme of flexible assembly by LST.

3D microscale surface of the underlying elastomeric substrate. Fig. 1 illustrates the fabrication process schematically. The laser-induced shockwave propagates through to-be-deformed laminated functional materials and provides sufficient momentum to achieve the conformal assembly with the underlying μ-patterned flexible substrates. The shockwave arises when the incoming laser pulse irradiates an ablation layer above functional materials and turns it into a plasma plume. The μ-patterns on the flexible substrates could be either replicated from rigid substrates multiple times by Polydimethylsiloxane (PDMS) replica molding process [12] or induced by pre-straining and oxygen plasma treatments [13]. The patterned microscale features are designed to mimic surface wrinkling in practical surface conditions during biological and biomedical transfer, which have been widely applied to tunable adhesion and wetting [14], tunable open-channel microfluidics [15], and stretchable electronics [16]. To minimize the mechanical damage to functional materials during deformation, they are encapsulated by symmetrical parylene layers and stay at mechanical neutral plane. The parylene layer not only absorbs most of shockwave energy, but also provides compliant media between functional layer and sharp microfeatures to mitigate the localized intensive deformation. A uniform nanolayer of adhesive (SU-8-2000, MicroChem®) will be spin-coated on the surface of encapsulated functional materials interfacing flexible substrates to improve the bonding strength during further transfers requiring stretching and bending. Another strategy to preserve the assembly functions is to differentiate plastic strains in ductile and brittle functional materials by patterned 3D surfaces. It is expected that metallic connections aligned to wavy regions will experience moderate plastic deformation, while the devices aligned with flat regions will have minimal plastic strains.

LST is a flexible and fast-shaping process suitable for meso-microscale 3D integration. The transferring process is ultrafast due to the nature of short pulse laser material interaction. During each pulse of laser beam (diameter 1–10 mm), the functional material could be faithfully transferred to 3D microscale surface of the underlying substrate within nanoseconds. In order to integrate large areas, laser beam could be operated in scanning mode. Given a specific configuration of confining media and ablation material, the laser pulse intensity, i.e. pulse energy averaged over beam size, determines the shockwave pressure. The laser intensity could be programmed to change instantaneously for different 3D microscale features and functional materials. The coded laser intensity also ensures high repeatability over multiple tests. The forming area, pending on laser beam size, could be changed in the range of few micrometers to millimeters. The laser pulse could readily scan over wafer-scale area or irradiate through mask to generate patterned shaping. The forming process could be considered to be athermal owing to the ablation and sacrifice layers above functional materials, which minimize thermal damage to functional materials. Compared with other stage-transfer techniques, it requires no complementary mold and reduces process complexity and cost. As the non-contact driving force, the shockwave has demonstrated its advantages in consistent mesoscale, microscale to nanoscale deformations conformal to the underlying 3D surfaces [17]. The conformal assembly of functional materials and the 3D microscale patterns (μ-patterns) has great potential to realize electronic systems more sensitive and responsive to environmental change.

III. Experimental Methods

Fig. 2 illustrates the experimental setup of LST to selectively fabricate stretchable functional structures conformal to 3D μ-patterns on the underlying elastomeric substrate. The laser pulse is provided by a Q-switched Nd:YAG laser in TEM00 mode and uniformed by a beam diffuser. It transmits through the top glass sample holder and irradiates the ablation

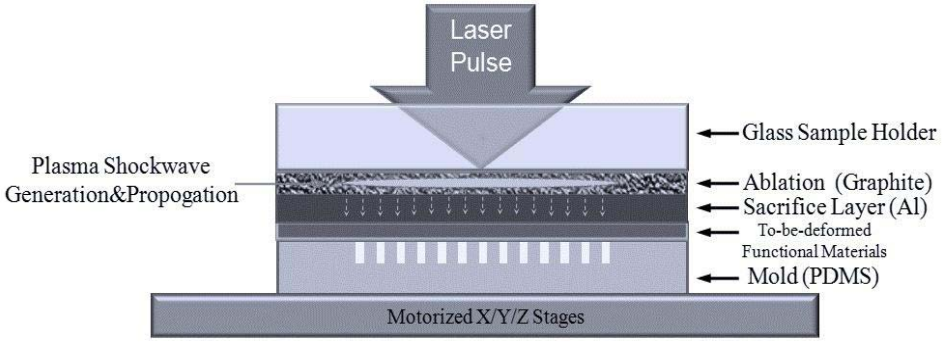

Fig. 2. The experimental setup of conformal flexible assembly by LST.

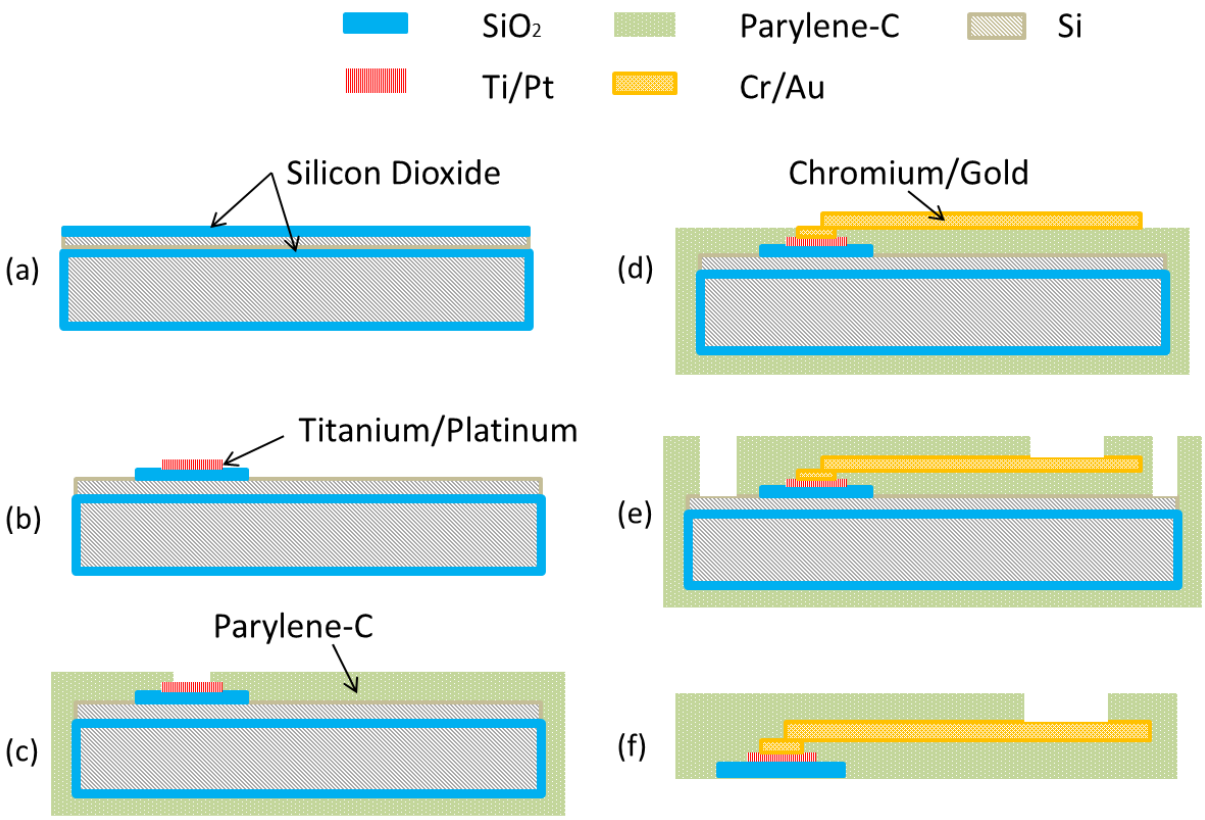

Fig. 3. Fabrication process of the shear stress sensor. (a) Thermal growth of SiO_2 and deposition of sacrificial Si layer (1 μm). (b) Deposition and patterning of Ti/Pt layers (0.12 μm /0.02 μm) for the sensing element. (c) Deposition of Parylene-C (9 μm). (d) Deposition and patterning of a metal layer of Cr/Au for electrode leads (0.6 μm). (e) Deposition and patterning of a thick layer of Parylene-C (12 μm) to form the device structure. (f) Etching the underneath Si sacrificial layer leading to the final device.

layer (graphite coating) into the plasma instantaneously. Confined by the sample holder, the plasma generates a transient shockwave which propagates through the aluminum sacrifice layer and the laminated functional materials and shapes them into structures conformal to the underlying 3D surfaces. The graphite ablation was sprayed onto the upper surface of aluminum sacrifice layer while the bottom surface interfaces with the laminated thin film, in order to prevent the graphite pollution and direct laser irradiation. The laminated thin film and 3D surface are bonded simultaneously by spin-coated adhesive on the interface. The magnitude of shockwave pressure is in the range of hundreds of MPa to several GPa, determined by laser intensity, shock impedance of confining media and ablation coating, as well as absorption coefficient of laser energy in plasma generation. In this study, shockwave pressure can be controlled by laser intensity solely to preserve the proper function of fabricated devices. The flexible PDMS substrates replicate μ-patterns in Si master molds faithfully by the method of mixing and curing the Dow Corning's Sylgard 184 elastomer kit at 80° for 90 mins before being peeled off from Si molds.

The functional laminates, such as shear stress sensor, was fabricated by surface micromachining of polymer Parylene-C. Parylene refers to a variety of chemical vapor deposited poly (p-xylene) polymers functioning as moisture and dielectric barriers. Among them, Parylene-C is most widely used considering its advantages in barrier properties, cost, and processing methods. In Fig. 3, the fabrication process includes: 1) dry thermal grow 0.3 μm thick SiO_2 on Si wafer, followed by deposition of 1 μm sacrificial silicon layer (polysilicon)

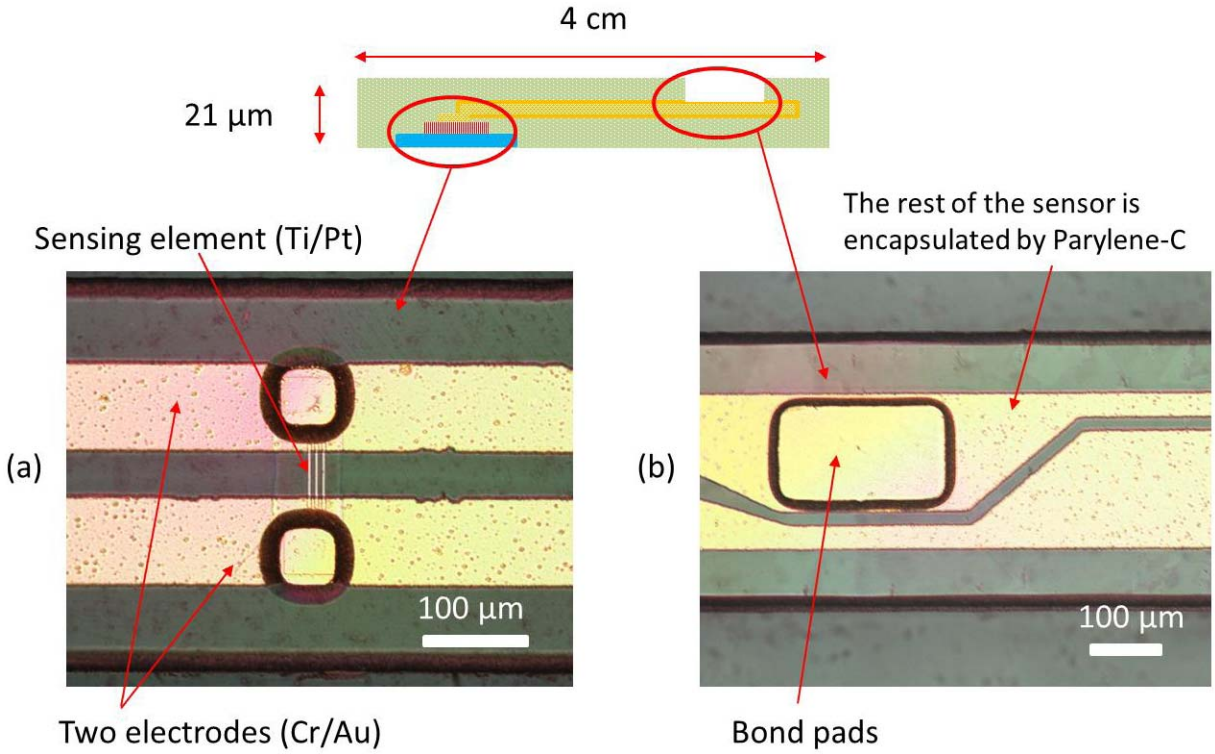

Fig. 4. Schematic of the shear stress sensor. (a) Sensing element; (b) Bond pads. The 3 lines bridging two electrodes are the sensing element, Ti/Pt layers with thickness of 0.12 μm/0.02 μm and patterned by lift-off to form a 2–3 μm wide metal traces [18].

through LPCVD. This layer will be etched completely during sensor releasing. Then, dry thermal grow approximately 0.2 μm SiO_2; 2) deposit Ti/Pt layers with thickness of 0.12 μm/0.02 μm for the sensing element with e-beam evaporator, and pattern these layers by lift-off to form a 2 μm to 3 μm wide metal traces; 3) deposit about 9 μm Parylene-C layer in the Parylene vacuum coating system and pattern this layer by oxygen plasma; 4) deposit and pattern a metal layer of Cr/Au for electrode leads (0.02 μm/0.6 μm); 5) deposit another layer of Parylene-C (12 μm) and pattern both Parylene-C layers to form the device structure; 6) etch the underneath silicon sacrificial layer through XeF_2 dry etching system, resulting in the final device. The overall sensor dimensions were 4 cm in length, 320 μm in width, and 21 μm in thickness, as illustrated in Fig. 4. We can also start from SOI wafers and skip the first two steps, but it may further increase the cost due to the higher unit price of SOI wafers.

IV. Results and Discussion

Fig. 5(a) shows the bending of a conformal assembly of a laminated shear stress sensor with a flexible PDMS mold, by the laser intensity of 0.25 GW/cm^2, with the zoom-in view in Fig. 5(b). In Fig. 5(c) and (d), it shows the images before and after LST of a laminated shear stress sensor on a flexible μ-patterned PDMS mold. In Fig. 5(d), the μ-patterns on the surface of PDMS mold, replicated from a master Si micromold, were faithfully transferred to the ductile connection of the sensor. The μ-pattern is 5 mm square in area, 160 μm in pitch width and 50 μm in depth. The sensor resistivity changed from 1.215KΩ to 1.292KΩ after LST and Temperature Coefficient of Resistance (TCR) was kept unchanged at approximately 0.11%/°C. The electrical resistance R of the metallic connection is determined by its length l, its cross-sectional area S, and the intrinsic resistivity ρ of the material: $R = \frac{\rho l}{S}$. The slight increase of sensor resistivity results from the longitudinal extension and the cross-section decrease of ductile metallic connections arising from the localized plastic deformation conformal to the μ-patterns. The deformation-induced microstructural defects, such as dislocations, will also contribute to the resistivity increase. The applied laser intensities and the aspect ratios of μ-patterns need to be controlled to avoid the fracture and failure of metallic connection. This method assumes that the parylene layer absorbs most of shockwave energy while providing a compliant soft substrate to the encapsulated functional layer. To validate this assumption, the laminated sensor was replaced by a 5 μm thick laminated thin film. Its cross section was fabricated by Focused Ion Beam (FIB) and characterized in Scanning Electron Microscope (SEM) in Fig. 5(e), showing its symmetric structures deposited on Si wafer. The thin film was deformed on another PDMS mold with wavy surface features and peeled off from PDMS substrate and characterized individually upside down in FIB in Fig. 5(f), since non-conductive PDMS substrate would deteriorate local ion beam cutting and observation if otherwise. Its cross section shows that, after laser-induced shock and deformation, the sandwiched Au layer keeps its thickness almost constant along the wave while parylene is subject to violent thickness changes, esp. in the layer interfacing PDMS mold. At the wave valley with sharp curvature, parylene thickness increases from 2.4 μm to 7.86 μm. The experimental observation reveals two underlying mechanisms coexisting to achieve uniform and significant

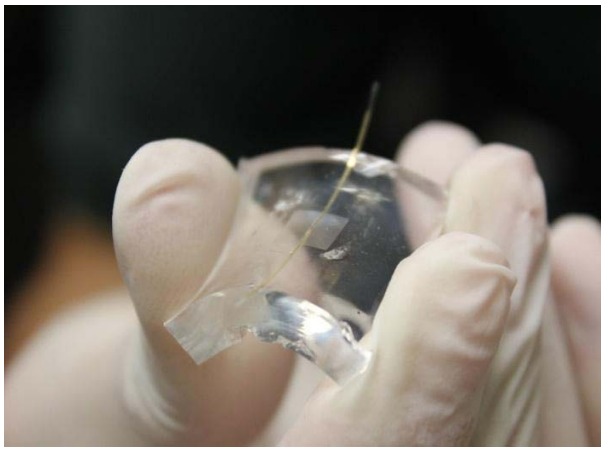

(a)

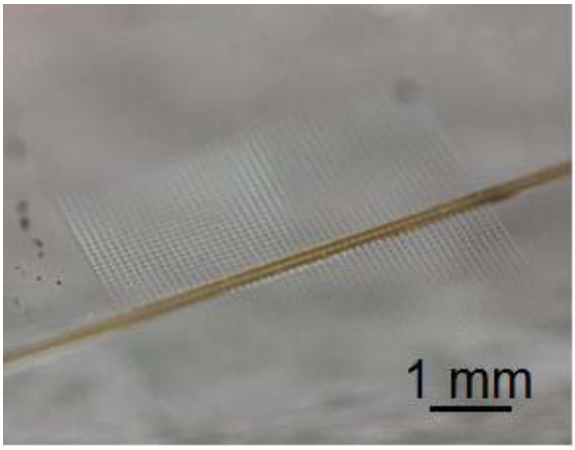

(b)

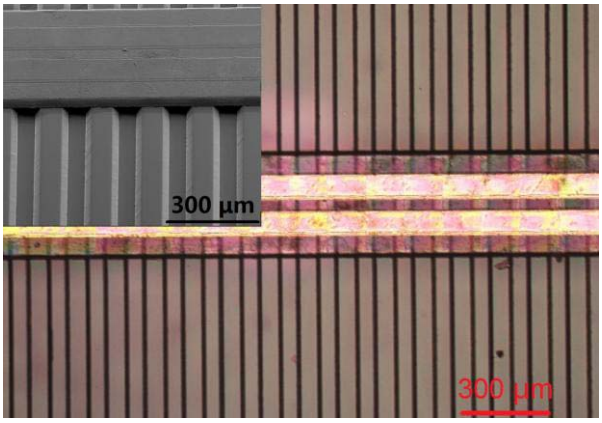

(c)

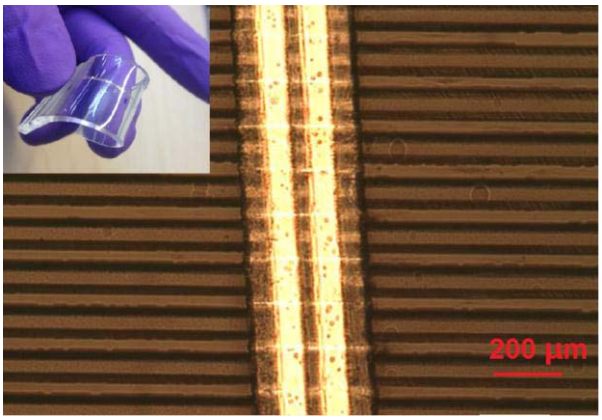

(d)

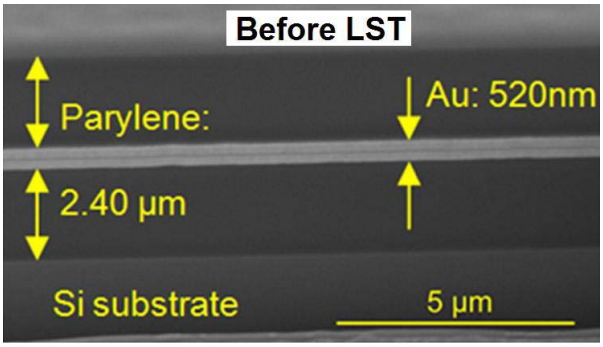

(e)

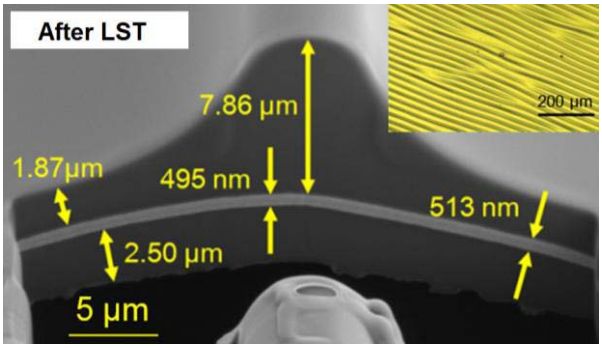

(f)

Fig. 5. (a) Bending of conformal assembly of a laminated shear stress sensor with a flexible PDMS mold, by the laser intensity of 0.25 GW/cm^2. (b) The zoom-in view of (a) demonstrates the structure after the sensor is transferred to the microscale pattern on the surface of PDMS mold. (c) The optical images shows the integration of sensor and PDMS micromold before LST (d) after transferring of a laminated shear stress sensor to a flexible μ-patterned PDMS mold. The laser intensity applied to make this assembly is 0.25 GW/cm^2. The SEM images of conformal assembly of laminated thin film with a wavy PDMS mold and the cross sectional view of the parylene layer and metallic connection layer (e) before and (f) after LST. After LST, the laminated thin film was peeled off from PDMS mold, then separately cut and characterized its convex "Lower Side" upside down in FIB/SEM. The applied laser intensity is 0.30 GW/cm^2.

plastic strain in functional layer. First, the encapsulation layer not only allows functional material to sustain large plastic strain, but also provides compliant media between functional layer and sharp microfeatures to mitigate the localized intensive deformation. More importantly, the permanent plastic deformation of parylene layer absorbs most of laser-induced shockwave energy. Second, the through-thickness compressive shockwave suppresses the debonding between parylene and Au layer so as to reduce the localized necking. It has been proved experimentally and analytically that the well-bonded metallic interconnections could sustain strains up to a few tens of percent without appreciable cracks since the localized necking could be suppressed by the adherent flexible substrate [19].

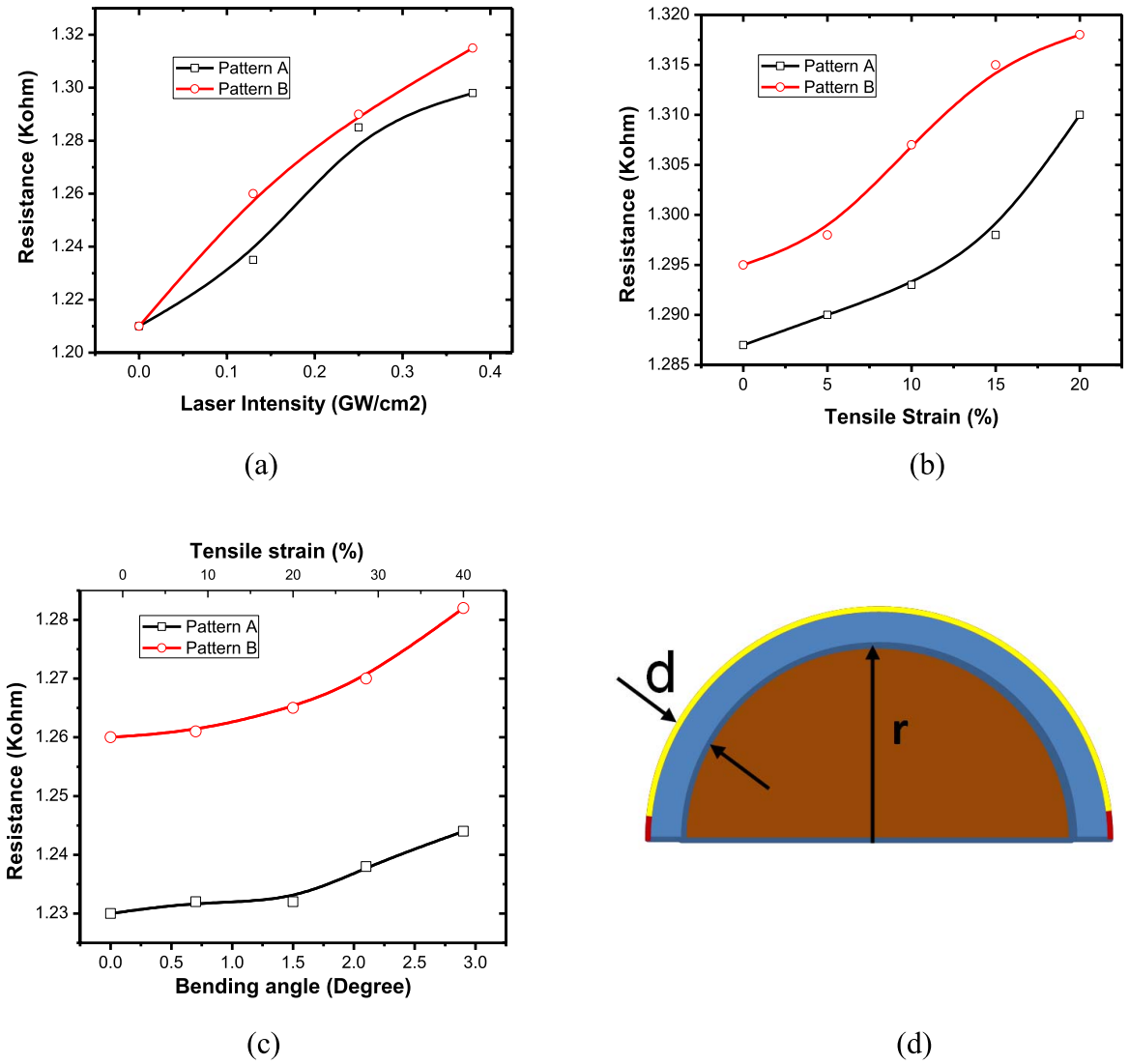

Fig. 6. The resistivity changes of shear stress sensors in the flexible assemblies: (a) due to the increasing laser intensities and aspect ratios of μ-patterns; (b) due to uniaxial stretching; (c) due to pure bending. The samples in (b) were fabricated by laser intensity: 0.25 GW/cm^2 in Group (a), and those in (c) by laser intensity: 0.13 GW/cm^2 in Group (a). In (d), d is the thickness of flexible assembly, which is approximately equal to the thickness of PDMS substrate since that of shear stress sensor is only 20 μm. r is the radius of cylindrical surface.

TABLE I
THE DIMENSIONS OF MICRO-PATTERNS REPLICATED INTO PDMS SUBSTRATE

Dimensions	Pattern A	Pattern B
Width (μm)	100	100
Depth (μm)	30	50
Aspect Ratio	0.3	0.5
Pitch (μm)	200	200

The applied laser intensities and the dimensions or aspect ratios of μ-patterns need to be controlled to avoid inducing excessive plastic strains or fractures to functional materials. In order to characterize their effects on the device functions, a batch of shear stress sensors were selected with the same initial electrical resistivity and deformed onto two different μ-patterns by the increasing laser intensities. The μ-patterns on the PDMS substrates have been displayed in Fig. 5(c) and the dimensions of μ-patterns summarized in Table I. The opening width of micro-trench in Pattern A is 100 μm, identical with that in Pattern B, while its depth in Pattern A is only 30 μm, less than that in Pattern B (50 μm). Given the same applied laser intensities, the metallic connection will be subjected to more longitudinal elongation, i.e. more plastic strains, in Pattern B with higher aspect ratio μ-patterns, which results in a slightly higher increase of sensor resistivity (See Fig. 6(a)). It is also observed in Fig. 6(a) that the resistivity increases with the applied laser intensities. It could be attributed to the increased microstructural defects arising from the higher laser-induced shockwave pressure. There is only a very slight resistivity change in the range of high laser intensities when the sensors have already approached localized

conformal deformations. When the applied laser intensity is sufficient to achieve the deformations conformal to microscale features, the excessive shockwave energy could result in more through-thickness compression of laminated structures.

The effect of overall tensile strains on flexible assemblies is demonstrated in Fig. 6(b), when they are subject to uniaxial stretching. In this study, the assemblies of shear stress sensor and PDMS substrate are chosen from the samples in Fig. 5(c) and (d), processed under laser intensity of 0.25 GW/cm^2. The PDMS substrates are stretched to experience the overall tensile strains of 5%, 10%, 15% and 20%, leading to the linear increase of resistivity approximately. The electrical resistivity changes induced by tensile stretching are found to be one order less than those introduced during assembly process. It is believed that during this macroscale stretching, the PDMS substrate undergoes uniform tensile strains while the localized tensile strain in the μ-patterns is reduced by the wrinkle-like microfeatures, which deform elastically to mitigate stretching in functional devices.

The effect of bending on functional assemblies is shown in Fig. 6(c). The assemblies, processed under laser intensity of 0.13 GW/cm^2 in Fig. 5(c), were wrapped onto the cylindrical surfaces with increasing curvatures, resulting in the increasing bending angles on the cylindrical surface. When the thickness of functional assemblies, d, is much less than the bending radius, r, the bending-induced tensile strain in laminated sensors could be approximated by $d/2R$. In this study, the thickness of flexible assembly is about 1 mm while the bending radii are in the range of 15–45 mm, resulting in the average tensile strains in the laminated sensors less than 7%. It shows that the resistivity of the functional assemblies increases consistently with curvatures and induced tensile strains. Further bending of functional assembly often results in the delamination of laminated sensors from flexible substrates.

V. Conclusion

In this study, we have demonstrated the process capability of LST to achieve the flexible and stretchable functional assemblies conformal to 3D μ-patterns in a fast-shaping and scalable way. The symmetrical elastomeric encapsulation of functional materials helps to extend the material formability and absorb most of laser-induced shockwave, preserving the device functions during conformal deformations. The effects of the applied laser intensities, μ-pattern designs, pure bending and uniaxial stretching over the flexible assemblies on the electrical resistivity of functional assemblies have been characterized. It shows that the device can sustain more than 40% strain in the stretchable substrate. The increase of resistivity arises from the longitudinal elongation and cross-section decrease along the conformal μ-patterned deformations, as well as the accumulated microstructural defects in the metallic conductive connections. The overall assembly process completes in nanoseconds at ambient temperature and pressure. Coupled with the inherent flexibility and scalability of laser processing, LST has the great potentials in the diversified applications needing flexible and stretchable electronics.

References

[1] A. Chirilă *et al.*, "Highly efficient Cu(In,Ga)Se2 solar cells grown on flexible polymer films," *Nature Mater.*, vol. 10, no. 11, pp. 857–861, 2011.

[2] T. Geller, "The promise of flexible displays," *Commun. ACM*, vol. 54, no. 6, pp. 16–18, 2011.

[3] K. Noda, H. Onoe, E. Iwase, K. Matsumoto, and I. Shimoyama, "Flexible tactile sensor for shear stress measurement using transferred sub-μm-thick Si piezoresistive cantilevers," *J. Micromech. Microeng.*, vol. 22, no. 11, p. 115025, 2012.

[4] K. Cherenack, C. Zysset, T. Kinkeldei, N. Münzenrieder, and G. Tröster, "Woven electronic fibers with sensing and display functions for smart textiles," *Adv. Mater.*, vol. 22, no. 45, pp. 5178–5182, Dec. 2010.

[5] H. Yu, L. Ai, M. Rouhanizadeh, D. Patel, E. S. Kim, and T. K. Hsiai, "Flexible polymer sensors for *in vivo* intravascular shear stress analysis," *J. Microelectromech. Syst.*, vol. 17, no. 5, pp. 1178–1186, Oct. 2008.

[6] J. A. Rogers, T. Someya, and Y. Huang, "Materials and mechanics for stretchable electronics," *Science*, vol. 327, no. 5973, pp. 1603–1607, 2010.

[7] T. Sekitani, Y. Noguchi, K. Hata, T. Fukushima, T. Aida, and T. Someya, "A rubberlike stretchable active matrix using elastic conductors," *Science*, vol. 321, no. 5895, pp. 1468–1472, 2008.

[8] X. Wang, H. Hu, Y. Shen, X. Zhou, and Z. Zheng, "Stretchable conductors with ultrahigh tensile strain and stable metallic conductance enabled by prestrained polyelectrolyte nanoplatforms," *Adv. Mater.*, vol. 23, no. 27, pp. 3090–3094, Jul. 2011.

[9] Y. Kim *et al.*, "Stretchable nanoparticle conductors with self-organized conductive pathways," *Nature*, vol. 500, no. 7460, pp. 59–63, 2013.

[10] X. Hu, P. Krull, B. de Graff, K. Dowling, J. A. Rogers, and W. J. Arora, "Stretchable inorganic-semiconductor electronic systems," *Adv. Mater.*, vol. 23, no. 26, pp. 2933–2936, 2011.

[11] D.-H. Kim, J. Xiao, J. Song, Y. Huang, and J. A. Rogers, "Stretchable, curvilinear electronics based on inorganic materials," *Adv. Mater.*, vol. 22, no. 19, pp. 2108–2124, 2010.

[12] T.-K. Shih, C.-F. Chen, J.-R. Ho, and F.-T. Chuang, "Fabrication of PDMS (polydimethylsiloxane) microlens and diffuser using replica molding," *Microelectron. Eng.*, vol. 83, nos. 11–12, pp. 2499–2503, 2006.

[13] C. de Menezes Atayde and I. Doi, "Highly stable hydrophilic surfaces of PDMS thin layer obtained by UV radiation and oxygen plasma treatments," *Phys. Status Solidi C*, vol. 7, no. 2, pp. 189–192, 2010.

[14] H. E. Jeong, M. K. Kwak, and K. Y. Suh, "Stretchable, adhesion-tunable dry adhesive by surface wrinkling," *Langmuir*, vol. 26, no. 4, pp. 2223–2226, 2010.

[15] K. Khare, J. Zhou, and S. Yang, "Tunable open-channel microfluidics on soft poly(dimethylsiloxane) (PDMS) substrates with sinusoidal grooves," *Langmuir*, vol. 25, no. 21, pp. 12794–12799, 2009.

[16] D.-Y. Khang, H. Jiang, Y. Huang, and J. A. Rogers, "A stretchable form of single-crystal silicon for high-performance electronics on rubber substrates," *Science*, vol. 311, no. 5758, pp. 208–212, 2006.

[17] H. Gao, R. Tang, T. Ma, H. Jiang, H. Yu, and G. J. Cheng, "Direct integration of functional structures on 3-D microscale surfaces by laser dynamic forming," *J. Microelectromech. Syst.*, vol. 22, no. 6, pp. 1428–1437, Dec. 2013.

[18] R. Tang, H. Huang, Y. M. Yang, J. Oiler, M. Liang, and H. Yu, "Three-dimensional flexible thermal sensor for intravascular flow monitoring," *IEEE Sensors J.*, vol. 13, no. 10, pp. 3991–3998, Oct. 2013.

[19] J. Wu *et al.*, "Stretchability of encapsulated electronics," *Appl. Phys. Lett.*, vol. 99, no. 6, p. 061911, 2011.

Huang Gao received the Ph.D. degree in industrial engineering from Purdue University, West Lafayette, IN, USA, in 2012, and the B.S. and M.S. degrees in mechanical engineering from Shanghai Jiao Tong University, Shanghai, China, in 2001 and 2004, respectively. His research focuses on micronanoscale fabrication, laser processing, and dynamic deformations. He was with GE Consumer & Industrial, Louisville, KY, USA, until 2007. He is currently a Senior System Development Engineer with Otis Elevator, Farmington, CT, USA.

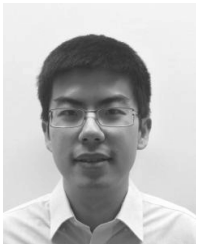

Rui Tang received the B.S. degree from the Huazhong University of Science and Technology, Wuhan, China, in 2009, and the M.S. degree from Arizona State University, Tempe, AZ, USA, in 2011, where he is currently pursuing the Ph.D. degree with the School of Electrical, Computer, and Energy Engineering. His current research includes the development of MEMS flow sensors, 3-D MEMS packaging, and flexible, stretchable, and foldable skins with integrated sensors and electronics.

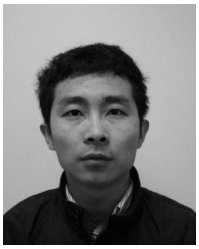

Teng Ma received the B.S. degree in thermal and power engineering from Xi'an Jiaotong University, Xi'an, China, in 2004, and the M.S. degree in mechatronics engineering from the University of Electronic Science and Technology of China, Chengdu, China, in 2009. He is currently pursuing the Ph.D. degree in mechanical engineering with the School for Engineering of Matter, Transport, and Energy, Arizona State University, Tempe, AZ, USA, where he is with Dr. Hanqing Jiang's Research Group. His research focuses on buckled stiff thin film on soft substrate for versatile functional materials, including anodes for lithium-ion batteries, optical gratings for microstrain sensors, and piezoelectric materials for energy harvesting devices.

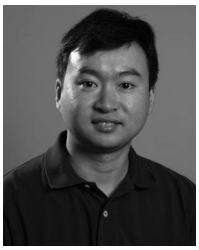

Hanqing Jiang is an Associate Professor in Mechanical and Aerospace Engineering with Arizona State University, Tempe, AZ, USA. He received the Ph.D. degree in solid mechanics from Tsinghua University, Beijing, China, in 2001, and was a Post-Doctoral Research Associate with the University of Illinois at Urbana–Champaign, Champaign, IL, USA, before joining Arizona State University in 2006. His current research interest is the multi-physics modeling and experiments for heterogeneous hard and soft materials.

Hongyu Yu received the B.S. and M.S. degrees from Tsinghua University, Beijing, China, in 1997 and 2000, respectively, and the Ph.D. degree from the University of Southern California, Los Angeles, CA, USA, in 2005. He holds the joint position between the School of Earth and Space Exploration and the School of Electrical, Computer, and Energy Engineering at Arizona State University, Tempe, AZ, USA. His research focuses on microelectromechanical systems for Earth and Space applications with an interest on microseismometer, harsh environment sensing, wireless sensing systems, flexible and stretchable electronics, and manufacture.

Gary J. Cheng received the Ph.D. degree in mechanical engineering from Columbia University, New York, NY, USA, in 2002. He is an Associate Professor with the School of Industrial Engineering and Mechanical Engineering by courtesy. He is a Fellow of the American Society of Mechanical Engineers. His research interests are scalable manufacturing of 0-D–3-D micro/nanostructures, laser matter interaction, and mechanical/physical property enhancement of materials.